MAGNETOHYDRODYNAMIC GO-WATER NANOFLUID FLOW AND HEAT TRANSFER BETWEEN TWO PARALLEL MOVING DISKS

by

Mohammadreza AZIMI and Rouzbeh RIAZI *

Faculty of New Sciences and Technologies, University of Tehran, Tehran, Iran

Original scientific paper
https://doi.org/10.2298/TSCI150713163A

The unsteady MHD squeezing flow of nanofluid with different type of nanoparticles between two parallel disks is discussed. The governing equations, continuity, momentum, energy, and concentration for this problem are reduced to coupled non-linear equations by using a similarity transformation. It has been found that for contracting motion of upper disk combined with suction at lower disk, effects of increasing absolute values of squeeze parameter are quite opposite to the case of expanding motion. In this case, radial velocity near upper disk decreases while near the lower disk an accelerated radial flow is observed. The comparison between analytical results and numerical ones achieved by forth order Runge-Kutta method, assures us about the validity and accuracy of problem.

Key words: *nanoparticle concentration, heat transfer enhancement, nanofluid, Brownian motion, approximate analysis*

Introduction

A nanofluid is achieved by dispersing nanoparticles in a base-fluid. Nanofluids, *i. e.* fluid suspensions of nanometer-sized solid particles and fibers, have been proposed as a route for surpassing the performance of heat transfer liquids currently available. Considerable attention has been recently given to nanofluids, nanoscale colloidal solutions, consisting of nanoparticles (with sizes of the order of 1 to 100 nm) dispersed in a base fluid [1, 2].

Nanofluid describe a fluid in which nanometer-sized particles are suspended [3]. Nanoparticles have unique properties, such as large surface area to volume ratio, and lower kinematic energy which can be exploited in various applications. Nanoparticles are more stable when dispersed in base fluids, due to their large surface area and they are more stable when compared to micro-fluids which lead to many practical problems. In recent years, nanofluids have attracted more and more attention.

There are four possible mechanisms in nanofluids contribute to thermal conduction: ballistic nature of heat transport in nanoparticles, Brownian motion of nanoparticles, liquid layering at the liquid/particle interface, and nanoparticle clustering in nanofluids. The Brownian motion of nanoparticles is too slow to directly transfer heat through nanofluid. However, it could have an indirect role to produce convection like micro-environment around the nanoparticles and particle clustering to increase the heat transfer [4, 5].

Heat transfer enhancement in various energy systems is vital because of the increase in energy prices. In recent years, nanofluids technology is proposed and studied by some researchers experimentally or numerically to control heat transfer in a process. The nanofluid can

* Corresponding author, e-mail: ro_riazi@ut.ac.ir

be applied to engineering problems, such as heat exchangers, cooling of electronic equipment, and chemical processes. Almost all of the researchers assumed that nanofluids treated as the common pure fluid and conventional equations of mass, momentum, and energy are used and the only effect of nanofluid is its thermal conductivity and viscosity which are obtained from the theoretical models or experimental data [6].

In various engineering problems, one may deal with mathematical relations which eventually reduce to equations in the form of ODE or PDE. In most cases, scientific problems are inherently of non-linearity that does not admit analytical solution, so these equations should be solved using special techniques. Some of these methods are reconstruction of variational iteration method [7], differential transformation method [8, 9], homotopy perturbation method [10], and optimal homotopy asymptotic method (OHAM) [11], and others [12-16].

The aim of this study is to investigate the MHD squeezing flow of nanofluid between parallel disks and illustrate the effect of different parameters on the results. We will also compare the analytical solutions with numerical ones in order to show the efficiency of the method.

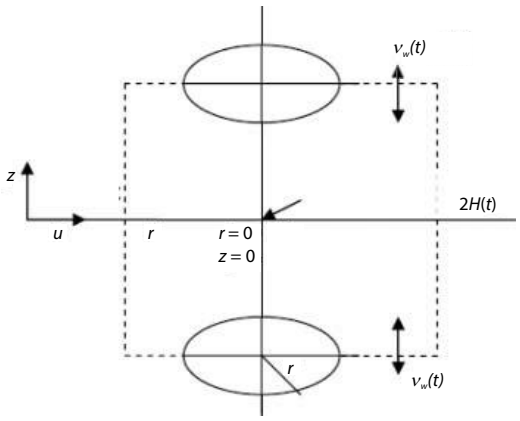

Figure 1. Physical model and co-ordinate system

Mathematical formulation

Figure 1 shows the geometry of the squeezing flow of an incompressible viscous MHD nanofluid between two circular plates separated by a distance $z = \pm l(1 - \alpha t)^{1/2} = \pm h(t)$. A uniform magnetic field of strength $B(t) = B_0(1- \alpha t)^{-1/2}$ is applied perpendicular to the disks. The upper disk at $z = h(t)$ approaching the stationary lower disk with the velocity $\mathrm{d}h/\mathrm{d}t$, whereas the flow is assumed to be axisymmetric with respect to $r = 0$. The velocity components along the radial and axial directions are $u(r, z, t)$, $w(r, z, t)$, respectively. Considering unsteady axisymmetric flow with negligible tangential velocity component, the conservation equations become:

$$\frac{\partial u}{\partial r}+\frac{u}{r}+\frac{\partial w}{\partial z}=0 \tag{1}$$

$$\rho_{\mathrm{nf}}\left(\frac{\partial u}{\partial t}+u\frac{\partial u}{\partial r}+w\frac{\partial u}{\partial z}\right)=-\frac{\partial p}{\partial r}+\mu_{\mathrm{nf}}\left(\frac{\partial^2 u}{\partial r^2}+\frac{\partial^2 u}{\partial z^2}+\frac{1}{r}\frac{\partial u}{\partial r}-\frac{u}{r^2}\right) \tag{2}$$

$$\rho_{\mathrm{nf}}\left(\frac{\partial w}{\partial t}+u\frac{\partial w}{\partial r}+w\frac{\partial w}{\partial z}\right)=-\frac{\partial p}{\partial z}+\mu_{\mathrm{nf}}\left(\frac{\partial^2 w}{\partial r^2}+\frac{\partial^2 w}{\partial z^2}+\frac{1}{r}\frac{\partial w}{\partial r}\right) \tag{3}$$

$$\frac{\partial T}{\partial t}+u\frac{\partial T}{\partial r}+w\frac{\partial T}{\partial z}=\frac{k_{\mathrm{nf}}}{\left(\rho C_p\right)_{\mathrm{nf}}}\left(\frac{\partial^2 T}{\partial r^2}+\frac{\partial^2 T}{\partial z^2}+\frac{1}{r}\frac{\partial^2 T}{\partial z^2}\right)+$$
$$+\tau\left\{D_B\left(\frac{\partial C}{\partial r}\frac{\partial T}{\partial r}+\frac{\partial C}{\partial z}\frac{\partial T}{\partial z}\right)+\frac{D_T}{T_m}\left[\left(\frac{\partial u}{\partial x}\right)^2+\left(\frac{\partial u}{\partial y}\right)^2\right]\right\} \tag{4}$$

$$\frac{\partial C}{\partial t}+u\frac{\partial C}{\partial r}+w\frac{\partial C}{\partial z}=D_B\left(\frac{\partial^2 C}{\partial r^2}+\frac{1}{r}\frac{\partial C}{\partial r}+\frac{\partial^2 C}{\partial z^2}\right)+\frac{D_B}{T_m}\left(\frac{\partial^2 T}{\partial r^2}+\frac{1}{r}\frac{\partial T}{\partial r}+\frac{\partial^2 T}{\partial z^2}\right) \tag{5}$$

Here, T_w and C_w are the temperature and nanoparticles concentration at the lower disk while the temperature and concentration at the upper disk are T_h and C_h, respectively, u and w – the velocities in the r, and z-directions, respectively, p – the pressure, T – the temperature, C – the nanoparticle concentration, D_B – the Brownian motion coefficient, D_T – the termophoretic diffusion coefficient, T_m – the mean fluid temperature, and k – the thermal conductivity. The last term in the energy equation is the total diffusion mass flux for nanoparticles, given as sum of two diffusion terms [13]. The dimensionless parameter, τ, gives the ratio of effective heat capacity of the nanoparticle material to heat capacity of the fluid. Effective density (ρ_{nf}), the effective dynamic viscosity (μ_{nf}), effective heat capacity $(\rho_{\mathrm{nf}})_{\mathrm{nf}}$ and the effective thermal conductivity k_{nf} of the nanofluid are [17]:

$$\begin{aligned}
&\rho_{\mathrm{nf}}=\rho_f(1-\varphi)+\rho_s\varphi_s\\
&(\rho C_p)_{\mathrm{nf}}=(\rho C_p)_f(1-\varphi)+(\rho C_p)_s\\
&\mu_{\mathrm{nf}}=\frac{\mu_f}{(1-\varphi)^{2.5}}\\
&\frac{k_{ns}}{k_f}=\frac{k_s+2k_f-2\phi(k_f-k_s)}{k_s+2k_f+2\phi(k_f-k_s)}\\
&\nu_{\mathrm{nf}}=\frac{\mu_f}{\rho_{\mathrm{nf}}}
\end{aligned} \tag{6}$$

The relevant boundary conditions for the problem are:

$$\begin{aligned}
&z=h(t)\rightarrow u=0,\quad w=w_w=\frac{\mathrm{d}h}{\mathrm{d}t},\quad T=T_H,\quad C=C_h\\
&z=0\rightarrow u=0,\quad w=-\frac{w_0}{\sqrt{1-\alpha t}},\quad T=T_w,\quad C=C_w
\end{aligned} \tag{7}$$

Previous equations can be simplified by introducing following parameters:

$$\begin{aligned}
&u=\frac{\alpha r}{2\sqrt{1-\alpha t}}f'(\eta),\quad w=-\frac{\alpha H}{\sqrt{1-\alpha t}}f(\eta),\quad \eta=\frac{z}{H\sqrt{1-\alpha t}}\\
&\theta=\frac{T-T_H}{T_W-T_H},\quad B=\frac{B_0}{\sqrt{1-\alpha t}},\quad \varphi=\frac{C-C_h}{C_w-C_h}
\end{aligned} \tag{8}$$

The previous parameters are substituted into eqs. (2) and (3). Then the pressure gradient is eliminated from the resulting equations. We finally yield:

$$f^{(IV)}-S\left(\eta f'''+3f''-2ff'''\right)-\mathrm{Ha}^2 f''=0 \tag{9}$$

Using eq. (8), eqs. (3) and (4) are simplify to the following equations:

$$\theta''+\mathrm{Pr}\,S\left(2f\theta'-\eta\theta'\right)+\mathrm{Pr}\,Nb\theta'\varphi'+\mathrm{Pr}\,Nt\theta'^2=0 \tag{10}$$

$$\varphi''+\mathrm{Le}S\left(2f\varphi'-\eta\varphi'\right)+\frac{Nt}{Nb}\theta''=0 \tag{11}$$

With the following boundary conditions:

$$f(0)=A,\quad f'(0)=0,\quad f(1)=0.5,\quad f'(1)=0,\quad \theta(0)=\varphi(0)=1,\quad \theta(1)=\varphi(1)=0 \tag{12}$$

where S is the squeeze parameter, Pr – the Prandtl number, A – the suction/blowing parameter, Ha – the Hartmann number, Nb – the Brownian motion parameter, Nt – the thermophoretic parameter, and Le – the Lewis number which are defined:

$$S=\frac{\alpha H^2}{2\nu_f},\quad \mathrm{Pr}=\frac{\nu_f}{\alpha},\quad A=\frac{w_0}{\alpha H},\quad \mathrm{Ha}=\sqrt{\frac{\sigma B_0^2 H^2}{\nu}},\quad \mathrm{Le}=\frac{\nu}{D_e}$$
$$Nb=\frac{(\rho c)_s D_B (C_w-C_h)}{(\rho c)_f \nu},\quad Nt=\frac{(\rho c)_s D_T (T_w-T_h)}{(\rho c)_f T_m \nu} \tag{13}$$

It is important to note that $A > 0$ indicates the suction of fluid from the lower disk while $A < 0$ represents injection flow.

Solution procedure

The considered problem is a boundary value problem, and requires proper numerical solver. Most of the existing numerical solvers in MAPLE software are a combination of trapezoid or midpoint methods. Each of these basic schemes has its own characteristics. Methods implemented based on trapezoid method work efficiently for typical problems, however, midpoint based techniques are best suited for handling harmless end-point singularities. Fourth order Runge-Kutta method is a midpoint method which improves the Euler method by one order [11]. In this section, the normalized eqs. (9)-(11) that are coupled with the boundary conditions given in eq. (12) are solved numerically by Runge-Kutta method using MAPLE software. The most popular Runge-Kutta methods are fourth order. This is because, for the second order approaches, there are infinite numbers of versions. The following formulation is the most commonly used form, *i. e*. the forth order Runge-Kutta method:

$$y_{i+1}=y_i+\frac{1}{6}(k_1+2k_2+2k_3+k_4) \tag{14}$$

where

$$k_1=E(x_i,y_i) \tag{15}$$

$$k_2=E\left(x_i+\frac{1}{2}h,\quad y_i+\frac{1}{2}k_1h\right) \tag{16}$$

$$k_3=E\left(x_i+\frac{1}{2}h,\quad y_i+\frac{1}{2}k_2h\right) \tag{17}$$

$$k_4=E(x_i+h,\quad y_i+k_3h) \tag{18}$$

The fourth order Range-Kutta numerical solver is a simple and efficient candidate technique for differential equations and in most situations of interest this method represents an appropriate performance.

Results and discussion

Effects of different flow parameters on the velocity, temperature and concentration distributions are discussed in this section. The effects of increasing suction at lower disk on both axial and radial velocities are displayed in figs. 2 and 3, respectively. It is evident that increasing value of

suction strength results in higher absolute values of both the velocities. As increasing suction allows more fluid to flow near the lower disk therefore a decrease in boundary-layer thickness is expected.

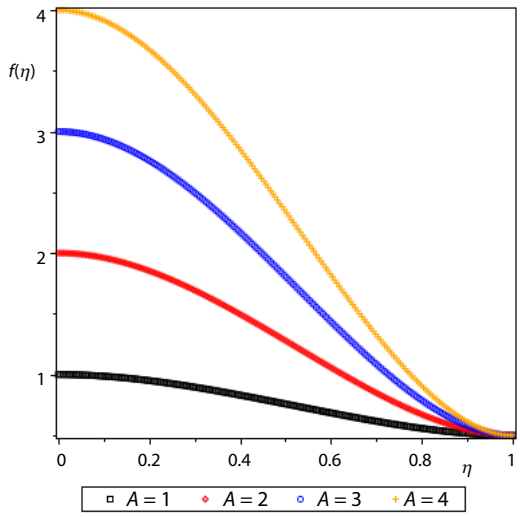

Figure 2. Effect of suction/blowing number on axial velocity in case of, Ha = 1, $S = 1$

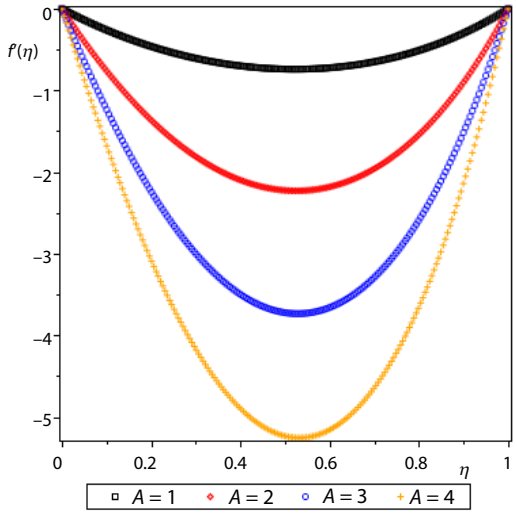

Figure 3. Effect of suction/blowing number on radial velocity in case of, Ha = 1, $S = 1$

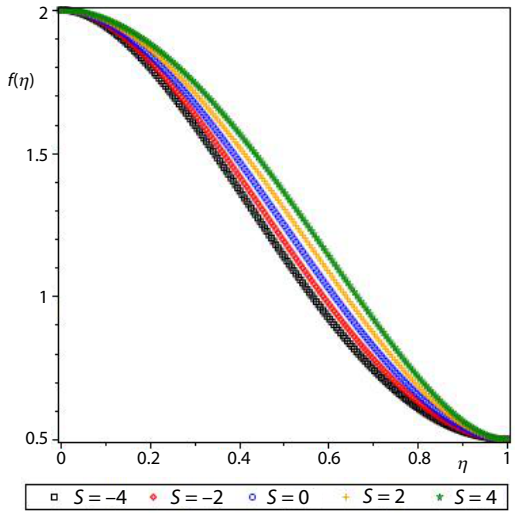

Figure 4. Effect of squeeze number on axial velocity in case of, Ha = 1, $A = 2$

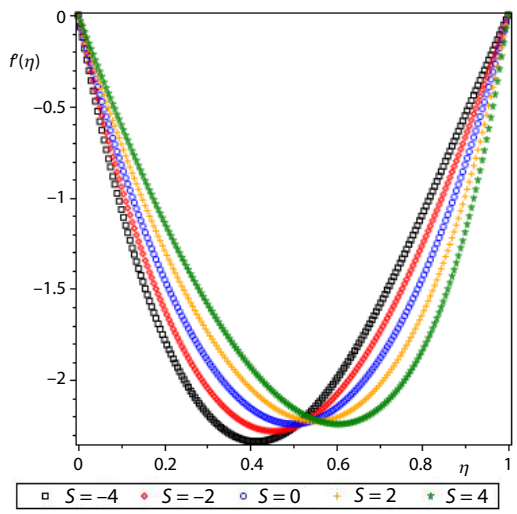

Figure 5. Effect of squeeze number on radial velocity in case of, Ha = 1, $A = 2$

Influences of squeeze parameter on axial and radial velocities are displayed in figs. 4 and 5, respectively. Here $S > 0$ denotes the movement of upper disk away from the lower disk. It can be seen from fig. 4 that for squeezing motion of upper disk combined with suction axial velocity near the center is increased while for dilating motion a decrease in axial velocity is observed. From fig. 5 one can see the behavior of radial velocity for same variations in S. It is evident for expanding motion; an accelerated radial flow is observed near the upper disk, however, this trend changes gradually as we move away from it. Somewhere near the center this trend gets converted into an opposite one, that is, from that point to lower disk a delayed motion

is observed. For contracting motion of upper disk, combined with suction at lower disk, effects of increasing values of squeeze parameter, S, are opposite to the case of expanding motion.

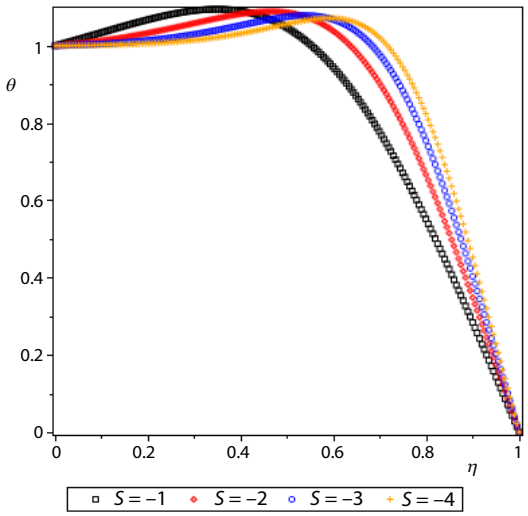

Figure 6. Effect of squeeze number on temperature in case of, Nb = 0.3, Nt = 0.2, Le = Ha = 1, Pr = 6.2, A = 0.5

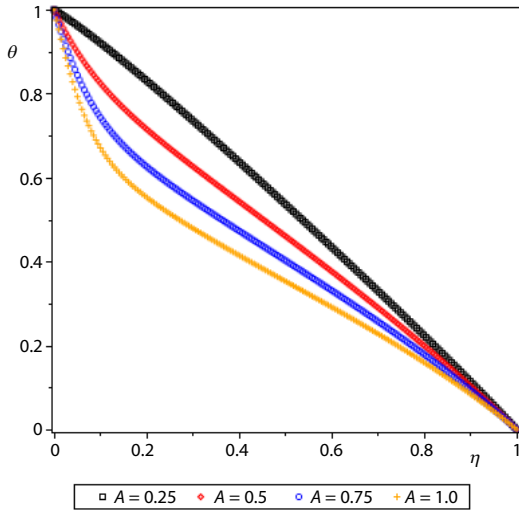

Figure 7. Effect of suction/blowing parameter on temperature in case of Nb = 0.1, Nt = 0.2, Le = Ha = S = 1, Pr = 6.2

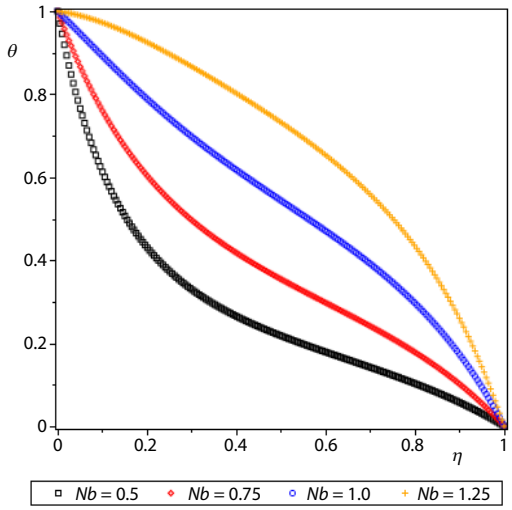

Figure 8. Effect of Brownian motion parameter on temperature in case of Nt = 0.1, Le = A = Ha = S = 1, Pr = 6.2

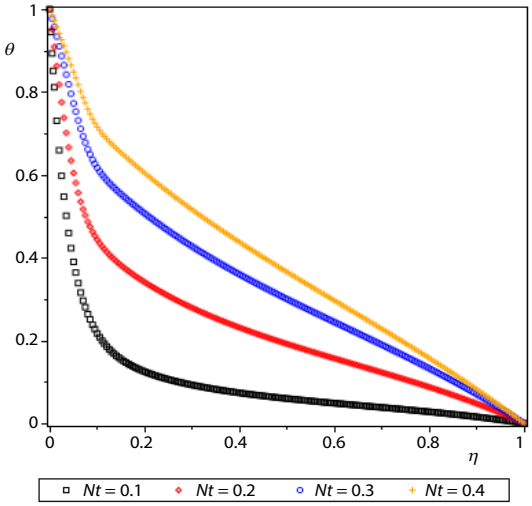

Figure 9. Effect of thermophoretic parameter on temperature in case of Nb = 0.1, Ha = 1 , Le = A = 1, S = 2, Pr = 6.2

The effects of interesting physical parameters, namely squeeze parameter, suction/blowing parameter, Brownian motion parameter, and thermoporetic parameter on the dimensionless temperature profile are sketched in the figs. 6-9.

The influence of squeeze number on temperature is illustrated in fig. 6. It can be seen from fig. 6 that the absolute of non-dimensional temperature increases for increasing S in the range of $0.5 < \eta < 1$.

Consequence of increasing suction parameter is presented in fig. 7 whereas the temperature reduces with increasing A. In another word, the temperature and thermal boundary-layer thickness are enhanced when we decrease the value of suction/blowing number.

Table 1 illustrates the effects of Hartmann number on the squeezing flow of nanofluid. The comparison of approximate (analytical) results [17] with numerical solutions obtained by fourth order Runge-Kutta, in the current study, have been also presented in case $A = -1$, $S = -1$, $Nb = 2$, $Nt = 0.1$, Le = 1, Pr = 6.2.

Table 1. Effect of Hartmann number on f

Ha	η	f_{num}	$f_{GOHAM[17]}$
1	0.1	0.25466	0.25129
	0.5	0.65183	0.64933
	0.8	0.38745	0.38548
3	0.1	0.23245	0.23567
	0.5	0.62946	0.62877
	0.8	0.39546	0.39222

Conclusions

This article investigates MHD squeezing flow of graphene oxide water nanofluid between parallel disks. At first the mathematical formulation is presented. Governing PDE are converted via similarity transformations. The numerical solution of governing equations were compared with analytical results previously obtained by using Galerkin OHAM method [17].

The following concluding remarks are achieved.

- The suction parameter decreases the thermal boundary-layer thickness hence at the disks we have higher rate of heat transfer.
- The effect of squeeze number on the axial velocity profiles is minimal.
- For contracting motion of upper disk combined with suction at lower disk, effects of increasing absolute values of squeeze number are quite opposite to the case of expanding motion. In this case, radial velocity near upper disk decreases while near the lower disk an accelerated radial flow is observed.
- For both the cases of suction and injection, the temperature and concentration function values increases monotonically as the similarity variable, A, increases.
- The axial component of velocity increases near the central axis of the channel but deceases near the walls.
- The transverse magnetic field decreases the fluid motion.
- The temperature significantly rise and profiles move closer to upper disk as Brownian motion parameter increase in both suction and blowing cases.
- Increasing Brownian motion parameter enhances nanoparticle concentration value.

A numerical solution using well known forth order Runge-Kutta method has also been obtained for the sake of comparison. It is found that the numerical and analytical results are in good agreement.

References

[1] Saidur, R., *et al*., A Review on Applications and Challenges of Nanofluids, *Renewable and Sustainable Energy Reviews*, *15* (2011), 3, pp. 1646-68

[2] Bahiraei, M., A Comprehensive Review on Different Numerical Approaches for Simulation in Nanofluids: Traditional and Novel Techniques, *Journal of Dispersion Science and Technology*, *35* (2014), 7, pp. 984-996

[3] Azimi, M., Riazi, R., Heat Transfer Analysis of Magnetohydrodynamics Graphene Oxide-Water Nanofluid Flow through Convergent-Divergent Channels, *Journal of Computational and Theoretical Nanoscience, 13* (2016), 1, pp. 659-665

[4] Azimi, M., Azimi, A., Flow Simulation of GO Nanofluid in Semi Porous Channel, *Turkish Journal of Science and Technology, 9* (2014), 1, pp. 67-72
[5] Azimi, M., Ommi, F., Using Nanofluid for Heat Transfer Enhancement in Engine Cooling Process, *Nano Energy and Power Research*, *2* (2013), 2, pp. 1-3
[6] Sheikholeslami, M., *et al*., Numerical Simulation of Two Phase Unsteady Nanofluid Flow and Heat Transfer between Parallel Plates in Presence of Time Dependent Magnetic Field, *Journal of the Taiwan Institute of Chemical Engineers, 46* (2015), Jan., pp. 43-50
[7] Azimi, A., Azimi, M., Analytical Investigation on 2-D Unsteady MHD Viscoelastic Flow between Moving Parallel Plates Using RVIM and HPM, *Walailak Journal of Science and Technology, 11* (2014), 11, pp. 955-963
[8] Ganji, D. D., Azimi, M., Application of DTM on MHD Jeffery Hamel Problem with Nanoparticles, *U.P.B. Scientific Bulletin Series A, 75* (2013), 1, pp. 223-230
[9] Sheikholeslami, M., *et al*., Application of Differential Transformation Method for Nanofluid Flow in a Semi-Permeable Channel Considering Magnetic Feild Effect, *International Journal of Computational in Engineering Science and Mechanics, 16* (2015), 4, pp. 246-255
[10] Azimi, M., Azimi, A., Investigation on the Film Flow of a Third Grade Fluid on an Inclined Plane Using HPM, *Mechanics and Mechanical Engineering, 18* (2014), 1, pp. 251-256
[11] Azimi, M., *et al*., Investigation of the Unsteady Graphene Oxide Nanofluid Flow between Two Moving Plates, *Journal of Computational and Theoretical Nanoscience, 11* (2014), 10, pp. 2104-2108
[12] Azimi, M., Ganji, D. D., Application of Max Min Approach and Amplitude Frequency Formulation to the Nonlinear Oscillation Systems, *The Scientific Bulletin Series A*, *74* (2012), 3, pp. 131-140
[13] Ganji, D. D., *et al*., Energy Balance Method and Amplitude Frequency Formulation Based of Strongly Non-Linear Oscillator, *Indian Journal of Pure & Applied Physics, 50* (2012), 9, pp. 670-675
[14] Azimi, M., Riazi, R., Analytical Simulation of Mixed Convection between Two Parallel Plates in Presence of Time Dependent Magnetic Field, *Indian Journal of Pure & Applied Physics*, *54* (2016), 5, pp. 327-332
[15] Azimi, M., *et al*., Analytical Investigation of MHD Jeffery Hamel Problem with Graphene Oxide Nanoparticles Using GOHAM, *Journal of Computational and Theoretical Nanoscience, 12* (2015), 6, pp. 991-995
[16] Azimi, M., Riazi, R., Flow and Heat Transfer of MHD Graphene Oxide Water Nanofluid between Two Non-Parallel Walls, *Thermal Science*, *21* (2017), 5, pp. 2095-2104
[17] Azimi, M., Riazi, R., Heat Transfer Analysis of GO-Water Nanofluid between Two Parallel Disks, *Propulsion and Power Research, 4* (2015), 1, pp. 23-30

Paper submitted: July 13, 2015
Paper revised: May 21, 2016
Paper accepted: June 30, 2016